A novel microfluidic chip for on-site radiation risk evaluation

Journal:	*Analyst*
Manuscript ID	AN-ART-07-2024-000941.R1
Article Type:	Paper
Date Submitted by the Author:	10-Oct-2024
Complete List of Authors:	Takahashi, Kenta; Ibaraki University, Department of Biological Sciences Tamura, Takahiro; Gunma University, Division of Mechanical Science of Technology Yamada, Kosuke; Gunma University, Division of Mechanical Science of Technology Suga, Kaisei; Gunma University, Division of Mechanical Science of Technology Aoki, Yuri; Gunma University, Division of Mechanical Science of Technology Sano, Ryota; Gunma University, Division of Mechanical Science of Technology Koyama, Kentaro; Gunma University, Division of Mechanical Science of Technology Nakamura, Asako; Ibaraki University, Department of Biological Sciences Suzuki, Takaaki; Gunma University

A novel microfluidic chip for on-site radiation risk evaluation

Kenta Takahashi[1] ・Takahiro Tamura[2] ・Kosuke Yamada[2] ・Kaisei Suga[2] ・Yuri Aoki[2] ・ Ryota Sano[2] ・Kentaro Koyama[2] ・Asako J. Nakamura[1] ・Takaaki Suzuki[2]

[1] Department of Biological Sciences, Ibaraki University, Mito, Japan

[2] Division of Mechanical Science of Technology, Gunma University, Kiryu, Japan

✉ suzuki.taka@gunma-u.ac.jp

✉ asako.nakamura.wasabi@vc.ibaraki.ac.jp

Keyword γ-H2AX assay ・On-site ・Particle sorting ・Particle trapping ・High throughput

Abstract

This paper proposes a microfluidic chip for on-site radiation risk evaluation using immunofluorescence staining for the DNA double-strand break (DSB) marker, phosphorylated histone H2AX (γ-H2AX). The proposed microfluidic chip separates lymphocytes, the cells of the DNA DSB evaluation target, from whole blood based on their size and traps them in the trap structure. The subsequent DNA DSB evaluation, γ-H2AX assay can be performed on a chip, which saves space and simplifies the complicated operation of assay, which conventionally requires a large experimental space. Therefore, this chip will enable the biological effect evaluation of radiation exposure to be completed on-site. Bead experiments with samples containing 10 μm and 27 μm diameter beads showed that the proposed chip introduced the sample into the flow channel only by centrifugal force and passively separate the two types of beads by the structure in the flow channel. In addition, bead experiments showed that isolated 10 μm diameter beads were trapped in more than 95 % of the 1,000 Lymphocyte trap structures (LTS). The feasibility of the proposed method for on-site radiation risk evaluation was demonstrated through cell-based experiments which performing the γ-H2AX assay in human lymphoblastoid, TK6 cells. Experiment shows that LTSs on flow channel are capable of trapping TK6 cells, and γ-H2AX foci which are marker of DNA DSBs are

observed in TK6 cells on chip. Thus, the results suggest that the proposed microfluidic chip simplifies γ-H2AX assay protocol and provide a novel method to perform the assay on-site, which conventionally impracticable.

1 Introduction

There are concerns about the effects of radiation on the human body in nuclear accidents, nuclear and radiological terrorist attacks, work in space, and medical diagnoses using radiation such as computed tomography (CT). Evaluating and managing the risk of radiation exposure to human health is an important issue in such an environment where there is a risk of radiation exposure [1][2][3]. When an unexpected radiation incident occurs that increases the likelihood of mass individual exposure, there are two populations of patients: those who are truly exposed to radiation, injured or ill, and those who have minimal or no exposure but complain of psychological distress, referred to as anxious patients [1]. In such a situation, it is necessary to assess patients exposed to high levels of radiation that require proper medical care by dose triage so that medical institutions can take appropriate action without confusion. To distinguish patients that need medical care from a large number of anxious patients, rapid dose evaluation at the time of transport is important. In the event of a large number of exposed patients, high-throughput dose evaluation techniques are desirable for performing a large number of tests at one time, however, high-throughput equipment is often expensive and large, making it unsuitable for on-site inspections, and a compact and simple on-site dose evaluation method is currently required. Furthermore, in these days, space exploration is growing and concerns about radiation exposure of occupational and commercial astronauts are also growing. In space, the effects of high-energy cosmic radiation on living organisms are greater than on the ground, which is covered by the atmosphere and magnetic field [4]. Longer stays in space associated with lunar and Mars exploration will require periodic evaluation of radiation exposure[2]. In such isolated environment as space and the area of radiation incident, since there is no lab facility, portable automated dose evaluation methods are needed. For these reasons, radiation exposure evaluation methods that can be used in emergencies and / or isolated environment have been investigated, but methods for rapid and accurate analysis of large numbers of patients have not yet been established[1][5].

In performing triage, there is the concept of biological dosimetry as a method to measure the direct effects of radiation exposure, and there are various methods to estimate radiation dose by measuring biological effects such as DNA and chromosome changes caused by radiation exposure. Among them, the dicentric chromosome assay (DCA) was established in the 1960s and has been used to this day, and has been adopted by the International Organization for Standardization (ISO) [6][7] and the International Atomic Energy Agency (IAEA) [8]. Although due to its high analysis accuracy DCA is recognized as the gold standard, this method is not suitable for dose estimation in situations of large-scale exposure requiring rapid biological evaluation or in space, where there is no sufficient experimental environment, because it takes time to estimate doses after isolating lymphocyte cells in peripheral blood and culturing them for 2 days before analysis, and requires a researcher skilled to count DCAs for the analysis.

On the other hand, radiation induced DNA double-strand break (DSB) detection using phosphorylated histone H2AX (γ-H2AX) is recognized as a rapid and sensitive biological dosimetry method [9]. γ-H2AX assay is sensitive enough to detect radiation exposure of 1.2 mGy [10][11] and its results can be acquired in less than 24hrs. However, a series of operations such as sample pretreatment, immunostaining, and analytical work require cumbersome operations and a large experimental space. Especially, method of lymphocytes separation from peripheral blood for γ-H2AX assay is complicated process. A study that fully automated a series of tasks to improve throughput achieved processing of 3,000 samples per day, but required a lot of equipment and large experimental space for automation[12]. In addition, studies using flow cytometers to miniaturize experimental systems have achieved palm-sized instruments, but have not been able to achieve simplicity throughout the process because sample preparation such as lymphocyte separation and immunostaining must be done separately[13]. Brenner et al. has reported a high-throughput system using imaging flowcytometry (IFC) has succeeded in creating a relatively compact system, but because it uses existing IFC techniques, the amount of blood used for analysis cannot be reduced to a single drop, making it unsuitable for onsite [14][15]. Thus, it is still difficult at present to perform a series of γ-H2AX assays conveniently on-site[16][17] [18] and a novel method to enable on-site γ-H2AX assays are needed.

To solve these problems, we focused on microfluidic chip. Research and development of microfluidic chips called MicroTAS (Micro Total Analysis System) and Lab on a chip have been actively carried out for the purpose of evaluation by simple on-site operation. Microfluidic chips integrate various functions such as sensors, microfluidic channels, valves, and chambers, and have many advantages such as miniaturization of the experimental system, saving the amount of reagents, and shortening the reaction time. Among them, a number of research results on the isolation of specific cells from complex cell populations for bio-medical applications have been reported [19][20][21][22][23][24][25][26]. To realize the on-site γ-H2AX assay, simplifying the method of lymphocytes separation from peripheral blood is crucial.

Although there are various methods of blood cell separation such as using antibody, this study focused on a microfilter, which is one of the most classic methods to separate cells based on size and flexibility [27][28]. The microfilter structure that we designed is using the 2 to 5 μm of size difference between the lymphocytes and granulocytes targeted in this study and the other blood cells (monocytes, erythrocytes, and platelets).

In addition, simplification and automation of testing are also important to realize on-site assays. Especially in the case of exposure due to an unexpected accident, it is not easy to estimate the exposure area, and when the affected area is identified, rapid onsite testing must be performed in the absence of researchers.

Microfluidic chips that use centrifugal force as the driving force of the fluid, especially those called Lab on a Compact Disc (CD), have the advantage of simplifying, automating and parallelizing the operation compared to general microfluidic chips that use a syringe pump as the driving force of the fluid [29][30]. There are also previous studies that have succeeded in miniaturizing devices by using centrifugation, and there are also previous studies in the area of cell separation that have separated specific cells by combining them with magnetic force [31][32]. On the other hand, target cells of previous studies flow through to the outlet and are densely grouped in one outlet, while flow path and microfilter structure in this study are designed to separate target cell and align them for final immunofluorescence staining and focus counting. This eliminates the overlapping of cells, making the observed image clearer, and also aims to determine the position of cells for performing image analysis efficient with the aim of automating the analysis in the future.

By applying Lab on a chip and Lab on a CD techniques to the γ-H2AX assay technology, this study aims to apply the γ-H2AX assay to on-site radiation exposure evaluations in areas where radiation accidents occur, space stations, and radiological medical facilities. The proposed microfluidic chip uses centrifugal force as the driving force of the fluid to separate and trap lymphocytes from whole blood based on their size using microstructures (Fig. 1a). In addition, the subsequent γ-H2AX assay can be realized on the same chip, which saves space and simplifies the operation of the γ-H2AX assay, which requires a large experimental space and complicated operations. In this way, the biological effects of radiation exposure can be evaluated, which completes the on-chip sample preparation onsite before the fluorescence observation. Specifically, experiments were conducted with bead and cell samples to evaluate the cell separation and trapping performance of the fabricated microfluid chips and the introduction of cells into the flow channel by centrifugal force. In addition, the introduction of the reagent into the flow channel was evaluated for assay operations that require multiple reagent changes. Finally, the validity of the proposed method was evaluated on the fabricated chips, ranging from cell manipulation to γ-H2AX assay.

2 Materials and methods

2.1 Trapping Lymphocytes for γ-H2AX assay

Whole blood contains various blood cells of different sizes and at different concentrations, as shown in Table 1. To perform the γ-H2AX assay for radiation risk evaluation, it is necessary to isolate lymphocytes for analysis from the blood, and monocytes and other blood cells are unnecessary because they interfere with the analysis. Therefore, in this study, we propose a microfluidic chip to trap and isolate lymphocytes from whole blood based on the size of blood cells and perform analysis on the chip. For simplicity of operation and automation in the future, the centrifugal force generated by the rotation of the chip is used to introduce blood cells and drug solutions into the flow channel.

The schematic of the proposed chip is shown in Fig. 1a and the dimensions of the entire chip and each structure are shown in Figs. 1b, 1c and 1d. The proposed chip has an inlet and outlet, and there is a flow channel in between them (Fig1b). On the flow channel, there are two types of structures. One is the Lymphocyte trap structure (LTS) that isolates target lymphocytes and the other is the Monocyte trap structure (MTS) that isolates monocytes from the blood. Each trap structure is placed along the flow from inlet to outlet as shown in Fig. 1b to efficiently isolate lymphocytes from the blood. As shown in Fig. 1c and 1d, both MTS and LTS are designed with the same concept, they are cup-shaped structures with openings, exit, at the bottom. In the flow channel, since the entrance diameter of the structure is longer than exit, target blood cells are trapped by following the path line through the entrance to exit of the trap structure. Once a target cell is trapped, the exit of the structure is blocked, resulting in a single cell being trapped in the structure. Thus, the target cell of each trap structure is trapped and isolated from rest of the blood component and blood cells with smaller size. As mentioned above, both MTS and LTS are specifically designed to match the dimensions of the target blood cells. Fig. 1c shows the MTS, which was designed to trap only monocytes with a diameter of 20~30 μm with an entrance diameter of 30 μm, an exit diameter of 18 μm to allow most of non-monocytes to pass through, and a structural height of 80 μm to allow multiple monocytes to be trapped in single structure. Fig. 1d shows the LTS, which has an entrance diameter of 18 μm, an exit diameter of 9 μm, and a structural height of 20 μm, which is 5 μm higher than the diameter of the lymphocyte to prevent the lymphocyte from clogging the flow channel. Besides, due to the difference in height between the MTS and LTS structures, the monocytes that were not trapped by the MTS are isolated at the boundary of the flow channel in front of the LTS. Red blood cells and platelets, which are smaller in diameter than white blood cells, pass through the MTS and LTS and are discharged to the outlet. Through the process above, once the single drop of blood dropped into the inlet, proposed chip separate and align the lymphocyte on LTS. Fig. 1e and 1f schematically illustrate the monocyte isolation and trapping lymphocyte described above from the top and cross-section of the chip.

Table 1 Blood components.

Cell type	White blood cell					Erythrocyte	Platelet
	Monocyte	Lymphocyte	Eosinophil	Neutrophil	Basophils		
Form							
Number of cell [cell/μl]	200~700	1500~3000	100	3000~5000	~70	$5x10^{6}$	$1.5x10^{5}$~$4x10^{5}$
Size [μm]	20~30	10~15	13~17	12~15	10~15	7~8	2~4
White blood cell [%]	3~5	20~40	2~5	50~70	~1		

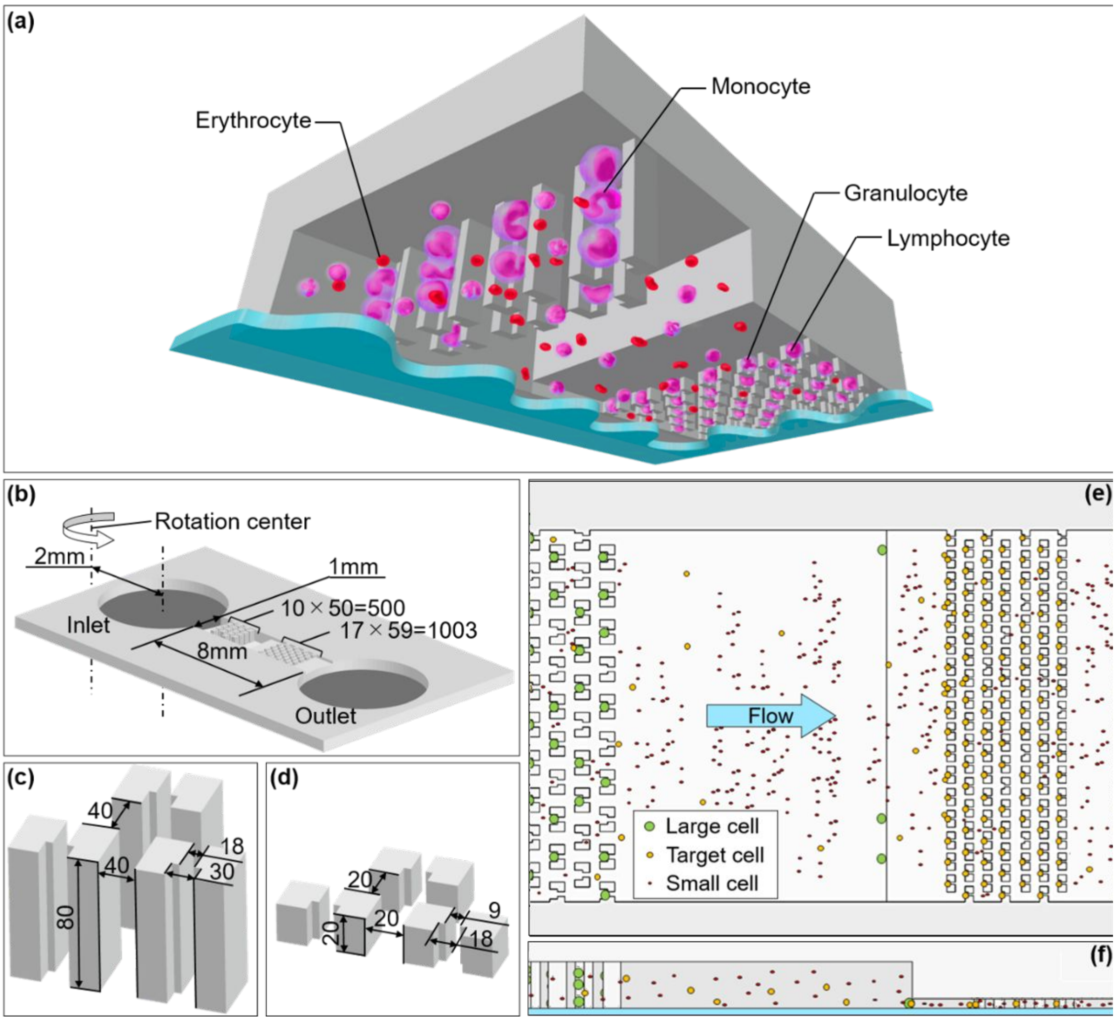

Fig. 1 Principle of lymphocyte isolation. (a) Schematic of the lymphocyte isolation chip. There are two types of structures in a single channel: the MTS on the upstream side of the channel for the isolation of monocytes, which are large cells, and the LTS on the downstream side of the channel for the isolation of lymphocytes, which are target cells. (b) Design of the lymphocyte isolation chip. (c) Schematic of a MTS. 500 MTSs are arranged on the upstream side of the channel. The unit is a micrometer. (d) Schematic of a LTS. 1003 LTSs are arranged on the downstream side of the flow channel. The unit is a micrometer. € Top view of lymphocyte isolation in the microchannel. Green circles represent monocytes, yellow circles represent target lymphocytes and granulocytes of comparable size to lymphocytes, and red circles represent erythrocytes and platelets. The number of blood cells in the figure does not

imitate the whole blood. (f) Cross-sectional view of lymphocyte isolation in the microchannel.

2.2 Device fabrication

The proposed chip was fabricated by soft lithography using a photoresist mold prepared by photolithography [33]. First, a 200 nm film of Cr was deposited on a glass substrate using a sputtering device (E-200S, Canon Anelva Corp., Japan), and a two-dimensional pattern of the LTS is transferred by the conventional photolithography. Then, a 20 μm thick film of negative photoresist SU-8 (3005, Nippon Kayaku Co., Ltd., Japan) was deposited on the Cr pattern using a spray coater (DC110, Nanotec Corp., Japan), and LTSs were fabricated by UV exposure from the backside of the glass substrate. Next, an 80 μm thick film of the SU-8 3005 was deposited on LTSs using the spray coater, and MTSs were fabricated by UV exposure from the top side of the glass substrate through a photomask aligned with the flow channel of the cell trap structure. Polydimethylsiloxane (PDMS, SILPOT 184, Dow Corning Toray Co., Ltd., Japan) chips were transferred by molding process using the photoresist molds obtained by the above process and bonded to a glass substrate by oxygen plasma using a reactive ion etching system (ES401, Nippon Scientific Co., Ltd., Japan) [34]. Figure 2 shows scanning electron microscopy (SEM, JCM-5700LV, JEOL Ltd., Japan) images of the PDMS chip before the bonding. MTSs made on the second layer are in upstream of the flow, and LTSs made on the first layer in downstream.

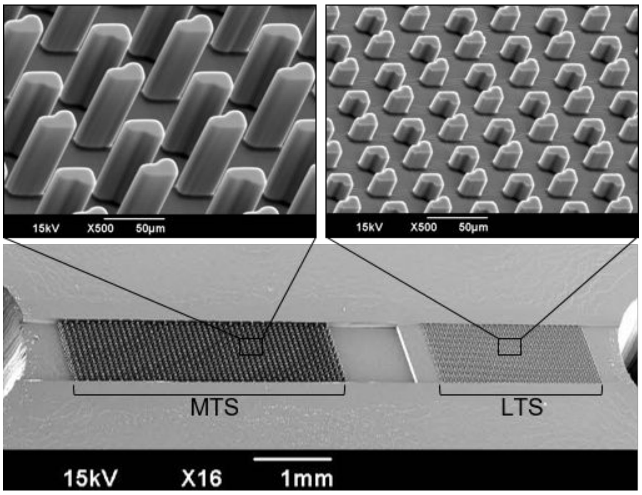

Fig. 2 SEM images of the fabricated chip. The lower image shows the entire chip, the upper left is an enlarged version of the MTSs, and the upper right is an enlarged version of the LTSs. Since monocytes are not a target of radiation exposure evaluation, the MTS structure has a relatively large aspect ratio so that multiple monocytes are trapped in the vertical direction of the structure. The LTS has a structural height as same as the tageted lymphocyte to trap single cell.

2.3 Sample preparation

Experiments evaluating trapping and isolation performance of trapping structures were performed using microbeads. The basic characteristics of the chip were evaluated by using microbeads with a uniform particle size as a substitute for the cells, and the practicality of the chip was evaluated by subsequent cell experiments. In the bead experiments, fluorescent bead suspension simulating blood was prepared by mixing two types of beads: beads with a particle size of 10 μm (G1000, Thermo Scientific, USA), corresponding to the target lymphocytes and granulocytes of similar size to lymphocytes, and beads with a particle size of 27 μm (35-5, Thermo Scientific, USA), corresponding to monocytes, which are large cells. To simulate the concentration of leukocytes in whole blood, the concentration of 10 μm beads was adjusted to 5×10^3 cells/μl assuming lymphocytes and granulocytes, and the concentration of 27 μm beads was adjusted to 3×10^2 cells/μl assuming monocytes. Experiments evaluating cell trapping performance and γ-H2AX assay were performed using cells. In the cell experiment, the cell sample was prepared with cultured human-derived lymphoblastoid (TK6 cells). TK6 cells were cultured in RPMI-1640 (R8658, Sigma-Aldrich, USA) containing 10 % fetal bovine serum (FBS, S1820-500, BioWest, France) at 37°C, CO_2 5%, and humidity over 90 % in an incubator (SCA-165DS, ASTEC, Japan). The cells were incubated in T-25 Flask (90025, Techno Plastic Products, Switzerland) for 4~5 days and passaged when they reached confluence. At the time of passaging, 8 ml of RPMI-1640 medium containing 10 % FBS warmed to 37°C was dispensed in advance into a new T-25 Flask, and 2 ml of TK6 cell suspension was re-seeded into it. The concentration of the cell sample was adjusted to approximately 5.0×10^3 cells/μl as the combined number of lymphocytes and granulocytes in human whole blood. TK6 cell samples were irradiated with 0.5 Gy, of X-rays to induce DNA damage (OM-B205, OHMiC, Japan).

2.4 Experimental procedure

The fabricated chips were degassed in a vacuum chamber to remove air bubbles in the flow channel. The flow channel was filled with pure water by dropping 5 μl of pure water into the inlet and outlet respectively to facilitate cleaning and introduction of the next drop of drug solution into the flow channel [35]. Drop 10 μl of the bead sample into the inlet and leave the chip in place for 5 min. Then, the chip was centrifuged for 30 s at an arbitrary rotation speed of 1000~3000 rpm using a tabletop centrifuge shown in Fig. 3a. The trapped beads were observed using an inverted microscope (IX-71, Olympus Corp. Japan) and a CCD camera (DP72, Olympus Corp. Japan). From the images obtained, the LTSs that trapped one or more beads were counted to determine the trapping efficiency. The trapping efficiency was calculated by dividing the number of LTSs that trapped beads of 10 μm diameter by the total number of LTSs. A larger trapping efficiency represents a higher percentage of structures trapping the target cell in the chip. The cell experiments were performed in the same way as the bead experiments described above, except that the chemical solution introduced as priming water was phosphate-buffered saline (PBS, T900, Takara Bio Inc., Japan).

2.5 Liquid replacement

The γ-H2AX assay to evaluate the biological effects of radiation exposure requires multiple injections of the chemical solution. The chip requires a liquid replacement operation that eliminates the chemical solution occupying the flow channel at each step and fills the flow channel with a new chemical solution. Therefore, the replacement performance of the chemical solution was evaluated using the liquid level difference between the inlet and outlet and the centrifugal force when the chip was rotated. We experimented under the three conditions: the standing only condition, the combined standing and centrifugal condition, and the combined multiple drops, standing and centrifugal conditions.

The fabricated chips were degassed in a vacuum chamber to remove air bubbles ©n the flow channel. The channel was filled with pure water by dropping 5 μl of pure water into the inlet and outlet. Assuming this state to be the initial state at time t = 0 min when the channel is filled with a certain chemical solution, we acquired fluorescence images of the channel. After that, any remaining pure water in the inlet and outlet was removed with a pipette. In the staining process of cells, since multiple drops of chemicals are dropped continuously, the chemicals accumulated in the inlets and outlets need to be removed each time. We dropped 10 μl of 0.5 mM uranine solution into the inlet and 5 μl into the outlet, respectively, and acquired fluorescence images in the channel at times t = 2, 5, and 10 min elapsed from the time the uranine solution was dropped. In the experiment under combined standing and centrifugal conditions, the chips were centrifuged at 1000 rpm for 30 s using the tabletop centrifuge after dropping the uranine solution using the same procedure as in the experiment under the standing only condition. The time when the chips were centrifuged was included in the time of liquid replacement, and the fluorescence images in the channel were acquired at the same elapsed time as in the standing only condition. In the experiment under combined multiple drops and standing and centrifugal conditions, images at time t =2 min are acquired using the same procedure as in the experiment under combined standing and centrifugal conditions. Then, the remaining chemical solution in the inlet and outlet was removed with a pipette, and again 10 μl of uranine solution was dropped into the inlet and 5 μl into the outlet. After that, the second centrifugation of the chips was performed under the same centrifugal conditions as the first, and images were acquired at time t = 5 and 10 min. After the fluorescence images were acquired, and the fluorescence intensity in the flow channel was acquired by using the image analysis software ImageJ.

2.6 γ-H2AX assay

The fabricated chips were degassed in a vacuum chamber to remove air bubbles in the flow channel. PBS was dropped into inlet and outlet. Thus, the flow channel was filled with PBS. Specifically, the chips were placed in a vacuum chamber (5305-0609, Thermo Scientific, USA), the air pressure in the chamber was reduced to -72 kPa using a vacuum pump (WP6210060, Gadner Denver, USA) connected to the chamber, and the chips were degassed at least 30 min under reduced pressure. Then, 10 μl of TK6 cell suspension was dropped into the inlet and the chips were centrifuged at 1000 rpm of rotation for 30 s using the tabletop centrifuge. The above cell suspension drops and centrifuge operations were repeated three times. To clean the flow channel, 10 μl of PBS was dropped into the inlet and the chips were centrifuged at 1000 rpm for 30 s using the tabletop centrifuge. Cells were fixed by dropping 2% PFA (paraformaldehyde) (163-20145, Wako, Japan) into the inlets and leaving the chips at room temperature for 20 min. After trapping the cells, to clean the flow channel, 10 μl of PBS was dropped into the inlet and the chips were centrifuged at 1000 rpm of rotation for 30 s using the tabletop centrifuge. To perform blocking, 5% BSA (Bovine serum albumin, A7184, Sigma-Aldrich, USA) / PBS was dropped into the inlet and allowed to react at room temperature for 1 hour. After blocking, 10 μl of PBS was dropped into the inlet to clean the channel. Then, 20 μl of anti–- γ-H2AX antibody solution (Alexa Flour® 488 anti-H2A.X Phospho (Ser139)) (613405, BioLegend, USA) diluted 200-fold dropped into the inlet, and the chips were centrifuged at 1000 rpm for 30 s using the tabletop centrifuge. The chips were left at room temperature for 2 hours and allowed to react with antigen-antibodies. To clean the flow channel, 10 μl of PBS was dropped into the inlet and the chips were centrifuged at 1000 rpm for 30 s using the tabletop centrifuge. This cleaning was repeated three times. Then, 30 μl of DAPI (4',6-diamidino-2-phenylindole) staining solution (H-1200, Vector Laboratories, USA) was dropped into the inlet. Finally, the sealing solution was dropped into the inlets and outlets and the inlets and outlets were sealed with a cover glass.

3 Results and discussion

3.1 Microbeads trapping experiment

To evaluate the cell isolation and trapping performance of the structure, experiments were performed on bead suspension simulating blood. The fluorescence images are shown in Fig. 3b. The number of beads was counted from the acquired images and a graph was created. Graphs for beads of 27 μm diameter and 10 μm diameter are shown in Fig. 3c and Fig. 3d, respectively.

The fluorescence image in Fig. 3b shows that the beads are isolated by two types of structures, indicating that the beads with a diameter of 10 μm are trapped in the LTS on the downstream side of the flow channel. Fig. 3d shows that the trapping efficiency was more than 95 % regardless of the rotation speed of the chip. The γ-H2AX assay requires at least 200 lymphocytes to evaluate the biological effects of radiation exposure to prevent data variability from affecting the evaluation. In this experiment, both lymphocytes and granulocytes were simulated with beads with a diameter of 10 μm. Therefore, considering that the ratio of lymphocytes to granulocytes in the blood is approximately 3:7, the number of lymphocytes obtained is approximately 950×0.3=285, which meets the target of 200.

Of the samples dropped into the inlet, only a small amount is introduced into the flow channel by centrifugation of the chip for 30 s, and many of the samples remain in the inlet after centrifugation. Since the centrifugal force increases with the rotation speed of the chip, the amount of sample introduced into the flow channel is also expected to increase. Fig. 3c shows the trapping efficiency of beads with a diameter of 27 μm trapped in the MTS when the rotation speed of the chip is changed, and the number of beads trapped in MTSs with a diameter of 27 μm increases with the rotation speed. It is assumed that the increase of the chip rotation speed also increased the number of beads introduced into the flow channel. However, the LTS on the downstream side of the flow channel was almost saturated with a trapping efficiency of more than 95 % at 1000 rpm of chip rotation, so no significant difference in the trapping efficiency was obtained even at higher rotational speeds. Fig. 3c shows that the number of 27 μm beads trapped in each line of MTS. Most of the 27 μm beads were trapped in the first 20 lines of MTS. There is no significant difference in the number of trapped beads between the rotation speed.

Considering the average number of trapped monocytes in the first 10 line is 7.4 and 200–- 700 monocytes are contained in 1 μl, it is estimated that 28–- 95 lines (280–- 950 MTSs) of MTS is sufficient to isolate most of monocyte in 1 μl of blood. Since the chip manufactured in this study has 500 MTSs in the flow path, it needs to be considered to increase the number of MTSs to isolate most of monocytes in 1 μl of blood.

This experiment showed that the centrifugal force generated by the rotation of the chip could introduce the cells into the flow channel. The results of the bead traps of the designed MTS and LTS showed that it is possible to passively isolate two different sizes of particles by structure. Furthermore, the designed LTS was found to have a shape suitable for trapping floating beads of similar size to lymphocytes.

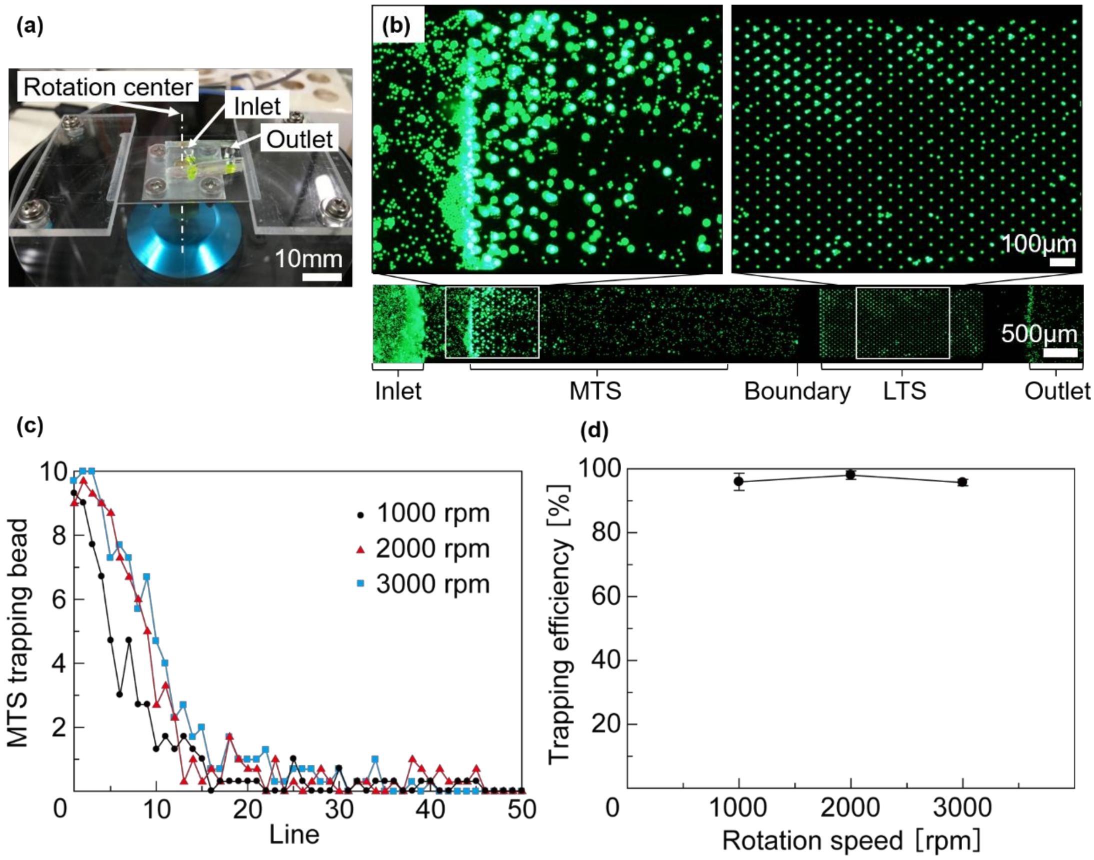

Fig. 3 Fluorescence observation images of the fluorescent bead separation trap experiment. (a) Photograph of the experimental system. The chip was fixed to a tabletop centrifuge with a jig. The sample or chemical solution was dropped into the inlet at the center of the chip to introduce into the flow channel by centrifugation. (b) Fluorescence observation image after centrifugation of the chip. The lower image shows the entire chip, the upper left image is an enlarged part of the MTS area, and the upper right image is an enlarged part of the LTS area. This figure was obtained from an experiment performed at a chip rotation speed of 1000 rpm. (c) The graph shows the distribution of beads with a diameter of 27 μm in the flow channel. The horizontal axis of the graph is the line order of MTSs from the inlet and the vertical axis is the number of MTSs trapping beads with a diameter of 27 μm (N=3). (d) The graph shows the relationship between the rotational speed of the chip and the trapping efficiency of beads with a diameter of 10 μm. The trapping efficiency is the percentage of LTS trapping beads with a diameter of 10 μm for 1000 LTSs (N=3).

3.2 Cell trapping experiment

Next, we evaluated cell separation and trapping performance of LTS using TK6 cells to simulate peripheral blood lymphocytes. The bright-field images are shown in Fig. 4a, and the experimental results analyzed from the obtained images are shown in Fig. 4b. The horizontal axis in Fig. 4b is the rotation speed of the chip and the vertical axis is the trapping rate of TK6 cells.

The bright-field image in Fig. 4a shows that the cells transported into the flow channel by centrifugal force are trapped in the LTS on the downstream side of the flow channel. This indicates that centrifugal force can be used to transfer cells to the flow channel and trap cells in the structure, similar to the bead experiments.

Although the trapping efficiency in this experiment was lower than the results of the bead experiment, Fig. 4b shows that a trapping efficiency of around 70 % was obtained regardless of the rotation speed of the chip, and considering that the ratio of lymphocytes to granulocytes (3:7), the number of lymphocytes obtained is approximately 700 × 0.3 = 210, which also meets the target of 200 as in the bead experiment. The reason for the low trapping efficiency of cell-based experiment compared to the bead experiment might be the flexibility of the cell. Considering the size of lymphocytes is about 9 to 12 μm in diameter, it is expected that most of lymphocytes can be trapped even at the exit width of 9 μm of the LTS. However, since lymphocytes are flexible enough to pass through capillaries of about 4 μm depending on the pressure, it is inferred that some of the lymphocytes passed through the 9 μm LTS exit and resulted low trapping efficiency [36]. In contrast, Polystyrene, the material of beads, is generally classified as a rigid plastic and has little flexibility, thus, bead experiment resulted in a higher trapping efficiency even with a 9 μm exit width [37].

In addition, in Fig. 4b, the variation of the experimental results increases as the rotation speed of the chip increases. The results of the experiment showed that average trapping efficiency in 2000 rpm is highest and in 3000 rpm, trapping efficiency decreased. With the increase of rotation speed, the splashing of the chemical from the inlet and the splitting of the chemical in the flow channel due to high centrifugal force is observed. We speculate that these factors contributed to the large variation in the trapping efficiency at the high rotation speed of the chip.

The cell trapping experiments showed that centrifugal force can be used to introduce cells into the flow channel and trap the cells in the LTS. We also consider that by designing the structure with consideration for the deformation of the cells, we can approach the high trapping efficiency in cell experiments as in bead experiments.

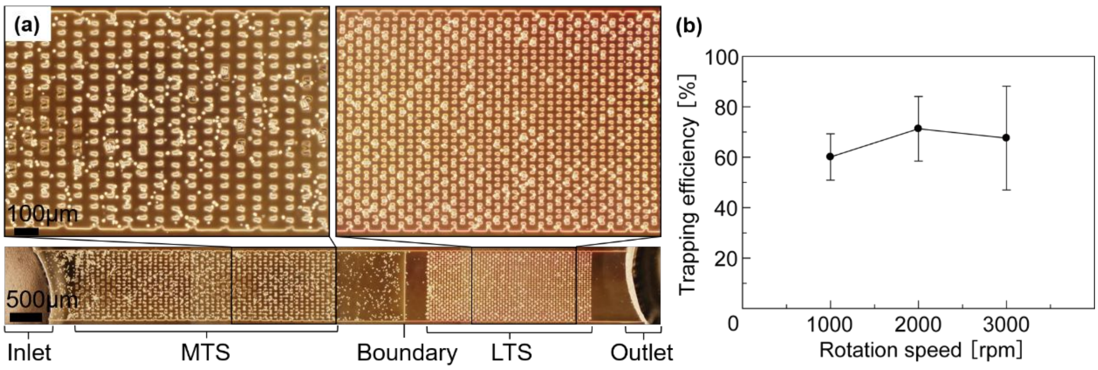

Fig. 4 Cell trapping experiment. (a) Bright field observation image of the chip after centrifugation. The lower image shows the entire chip, the upper left image is an enlarged part of the MTS area, and the upper right image is an enlarged part of the LTS area. This figure was obtained from an experiment performed at a chip rotation speed of 1000 rpm. (b) The graph shows the relationship between the rotation speed of the chip and the trapping efficiency of TK6 cells. The trapping efficiency is defined in the same way of the bead experiment (N=3).

3.3 Demonstration of liquid replacement using centrifugal force

In order to perform the γ-H2AX assay by introducing reagents into the captured cells, it is necessary to introduce and exchange fluids in the channel. To evaluate the effectiveness of centrifugation for fluid exchange in the channel, we compared the efficiency of fluid exchange under hydrostatic pressure (standing only condition) with that under combined centrifugation and hydrostatic pressure (standing and centrifugal conditions).

As an example of the experimental results, the fluorescence images obtained under the standing only condition are shown in Fig. 5a. The fluorescence intensity at each time was acquired at 0.2 and 2.7 mm along the x-axis in the bright-field images shown in Fig. 5a, and the average of the two locations was used as the fluorescence intensity at that time. Finally, the fluorescence intensity at each time was divided by the value of the fluorescence intensity in the channel of 0.5 mM uranine solution before introducing and the graph shown in Fig. 5b was prepared. In the figure, the black circle is for the standing only condition, the red circle is for the combined standing and centrifugal condition, and the blue square is for the combined multiple drops, standing and centrifugal conditions.

From the results of the standing only condition, fluorescence intensity in the channel is increasing with time and it suggests that it is possible to introduce the chemical solution by the difference of hydrostatic pressure between inlet and outlet under the gravity condition (Fig. 5b). The increasing rate of fluorescence intensity in the time between 0 to 2 minutes after drop is significantly higher under the standing and centrifugal condition combined compared to the standing only condition, and Fluorescence intensity under the standing only condition never reached 0.4 throughout the experiment while the standing and centrifugal condition reached 0.9 in 2 minutes (Fig. 5b). Therefore, the centrifugation of the chip is effective for the introduction and exchange of chemical solutions. In addition, as shown in the red and blue plots at t = 2 min in Fig. 5b, a single introduction of the chemical solution resulted in a concentration of approximately 90 % of the reference solution, and we estimate that the number of times of introduction in each process is sufficient for 1 to 2 times.

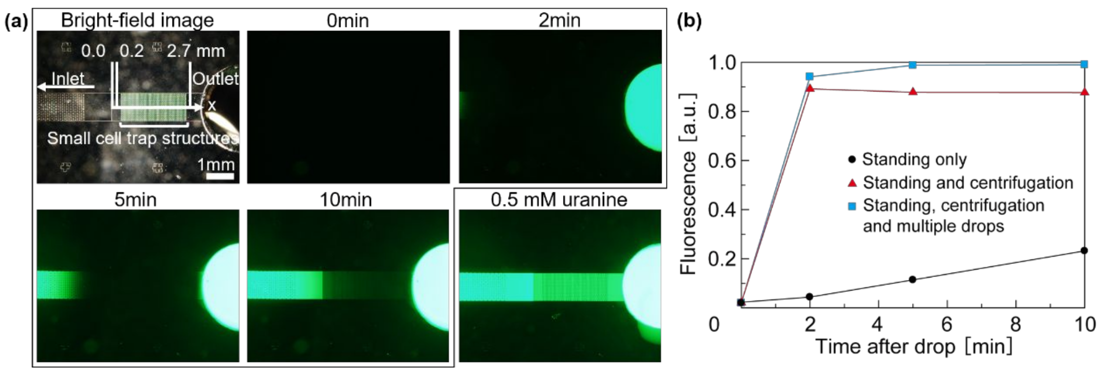

Fig. 5 Results of drug introduction experiment. (a) Observation image of drug introduction experiment. The image inside the black line is an observation image under the standing only condition, the upper left image is a brightfield observation before the experiment started, and the other images are fluorescence observations taken from the

start of the experiment over time. The lower right image is a graph of the observed fluorescence of 0.5 mM uranine solution, which was used as a reference for the experiment. (b) The graph shows the time course of the loading of the chemical solution, which is the fluorescence intensities of the uranine solution. Fluorescence intensities were obtained from the observed fluorescence images in the experiment using ImageJ, an image analysis software.

3.4 γ-H2AX assay

All operations were performed on the proposed chip, from the drop and introduction of cell suspension into the flow channel to the γ-H2AX assay. The TK6 cell samples were irradiated with 0.5 Gy X-ray to induce DNA double-strand breaks (DSBs).

The fluorescence images of LTS on the chip are shown in Fig. 6. Figs. 6a, b and c show the same part of the LTS on the same chip, and Figs. 6a', b' and c' are enlarged images of the same part. The liquid flow in the channel was generated from left to right in the image.

As shown in Fig.6a and 6'', blue fluorescence objects are observed in a regular pattern that similar to arrays of LTS. Therefore, Fig.6a and 6'' showed that LTS is capable of trapping and lining up lymphocyte.

Green fluorescence foci are observed in Fig.6b and 6b'. Although fluorescent antibodies specifically bind to γ-H2AX, occasionally they bind to non-specific protein. Since γ-H2AX is the histone protein and it located in nuclei, to clarify green foci are specific binding, merging γ-H2AX-image(green) with nucleus-image (red) is efficient (To enhance the contrast of two images we turned blue nucleus-image to red using imageJ).

As shown in Figs. 6c and 6'', green fluorescence foci are observed on the red circle indicating that green fluorescent foci in this image is γ-H2AX foci.

Hence, these results suggest that it is possible to perform the entire process from cell isolation to γ-H2AX assay on the proposed PDMS chip using centrifuge procedure. Since this experiment was conducted using only one type of cell, we plan to evaluate the performance of the proposed chip by using peripheral blood with multiple blood cells of different sizes.

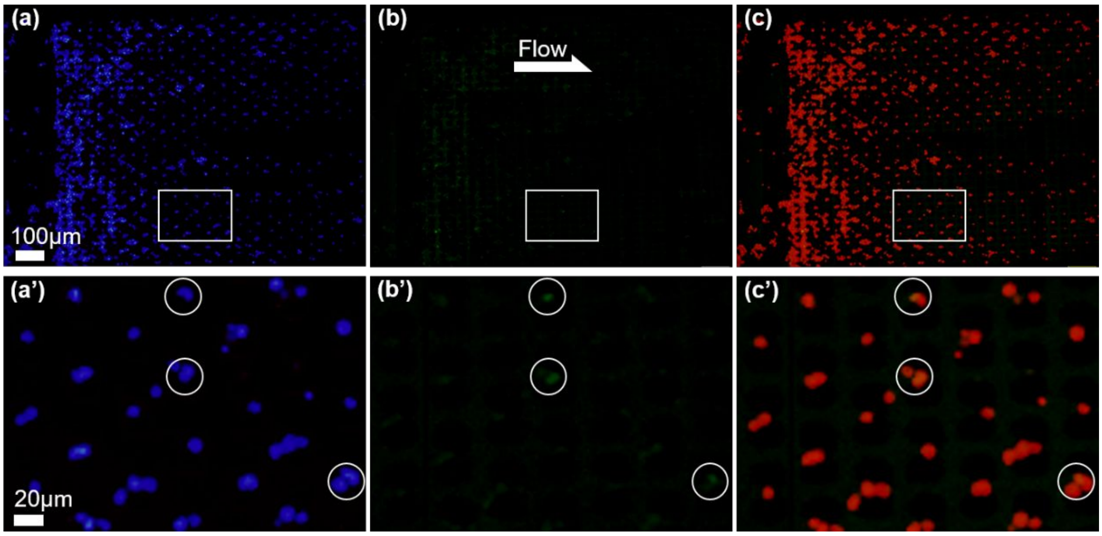

Fig. 6 Results of γ-H2AX assay of TK6 cells in experiments using the proposed chip. (a) Blue is the DAPI-stained cell nucleus. (b) Green is the fluorescence of the antibody bound to the DNA double-strand break marker γ-H2AX, indicating the site of DNA damage. (c) Merged fluorescent images of the cell nucleus and the site of damage. Red is the nucleus of the cell. Yellow is the DNA double-strand break site. Each image with a dash is an enlarged image within a white square in an unmarked image. The image shows that the staining process of cells trapped in the LTS can be performed in the chip.

4 Conclusions

To apply the γ-H2AX assay to on-site biological effects evaluation of radiation exposure, we developed a microfluidic chip to save space and simplify the operation of the γ-H2AX assay, which conventionally requires a complicated experimental system and operation.

In bead experiments, the centrifugal force on the rotating chip introduced beads into the flow channel, passively isolate particles by structure, and trap them into the structure. The trapping efficiency for the number of structures exceeded 95 %, indicating that the trapping efficiency is sufficient for the evaluation of the biological effects of radiation exposure. In cell experiments, the centrifugal force introduced cells into the flow channel and trap them into the structure. The trapping efficiency of TK6 cells was around 70 %

and it also reached more than 200 cells, which indicates that the chip is usable for trapping enough cells to perform γ-H2AX assay. On the other hand, using cell sample decreased trapping efficiency due to the flexibility of the cells. To improve the trapping efficiency, the opening width of LTS would be narrowed to prevent cells from passing through. In a liquid replacement experiment, the channel was filled with 90% of the concentration of the inflowed chemical solution at once. Finally, we demonstrated tγ-H2AX assay on the proposed chip by performing the entire process from the introduction of cell suspension to evaluate the DNA damage in the channel.

In addition, the microfluidic chip developed in this study enables the γ-H2AX assay to obtain the results in a shorter time than the assay using the conventional method. Conventionally, the process of separating lymphocytes, which are the target of analysis, takes about three hours, depending on the skill of the person conducting the experiment. In contrast, using the microfluidic chip, the time required for blood separation can be reduced to 30 seconds, 1/360 of the time required by the conventional method.

Moreover, the microfluidic chip reduces the amount of blood used for the γ-H2AX assay. Conventional γ-H2AX assays require 5 to 7 ml of blood, but using our method, 1 to 5 μl of blood is sufficient for analysis. These time savings and reduced blood volume are beneficial in the triage of accidentally exposed individuals who may unexpectedly require on-site γ-H2AX assays.

On the other hand, as for the accuracy of analysis, as shown in Fig. 6, the observation of γ-H2AX focus is possible, although it is thought that there is no significant difference in the accuracy of analysis, further validation is needed with the development of microfluidic chips optimized for cell samples.

These results suggest that the microfluidic chip developed in this study propose one novel method that allows γ-H2AX assays to be performed on-site. For future research, γ-H2AX assay against peripheral blood lymphocyte on the chip and establishment of LTS designs for with higher trapping efficiency will be needed. Furthermore, on-site γ-H2AX assay will be realized by developing an analysis device equipped with a unit that automatically drops reagents onto the current microfluidic chip and a unit that takes fluorescent images.

Acknowledgements

This research was partially supported by JSPS Science Research Grant 23H01363, 22H02105, JST CREST Grant Number JPMJCR19Q2, Gunma University for the promotion of scientific research and Grant Number 18H04964, Research on the Health Effects of Radiation organized by Ministry of the Environment, Japan.

References

[1] Rea ME, Gougelet RM, Nicolalde RJ, Geiling JA, Swartz HM, Proposed triage categories for large-scale radiation incidents using high-accuracy biodosimetry methods. Health Phys. 2010 Feb; 98(2):136-44.

[2] McKenna-Lawlor S, Bhardwaj A, Ferrari F, Kuznetsov N, Lal AK, Li Y, Nagamatsu A, Nymmik R h, Panasyuk M, Petrov V, Reitz G, Pinsky L, Shukor SM, Singhvi AK, Straube U, Tomi L, Townsend L, Feasibility study of astronaut standardized career dose limits in LEO and the outlook for BLEO. Acta Astronautica, 2014 Jul; 104(2):565-573,

[3] Mothersill C, Seymour CB, Radiation-induced bystander effects--implications for cancer. Nat. Rev. Cancer, 2004 Feb;4(2):158-64.

[4] Wakayama S, Kamada Y, Yamanaka K, Kohda T, Suzuki H, Shimazu T, Tada MN, Osada I, Nagamatsu A, Kamimura S, Nagatomo H, Mizutani E, Ishino F, Yano S, Wakayama T, Proc. Natl. Healthy offspring from freeze-dried mouse spermatozoa held on the International Space Station for 9 months. Acad. Sci. USA, 2017 Jun 6;114(23):5988-5993.

[5] Sullivan JM, Prasanna PGS, Grace MB, Wathen L, Wallace RL, Koerner JF, Coleman CN, Assessment of biodosimetry methods for a mass-casualty radiological incident: medical response and management considerations. Health Phys. 2013 Dec;105(6):540-54.

[6] ISO. Radiation protection - Performance criteria for service laboratories performing biological dosimetry by cytogenetics. ISO 19238. Geneva: ISO; 2004 Jul.

[7] ISO. Geneva, Radiation protection - Performance criteria for laboratories performing cytogenetic triage for assessment of mass casualties in radiological or nuclear emergencies - General principles and application to dicentric assay. ISO 21243. Geneva:

ISO; 2008 Sep

[8] IAEA. Cytogenetic Dosimetry: Applications in Preparedness for and Response to Radiation Emergencies. EPR-Biodosimetry. Vienna: IAEA; 2011 Sep.

[9] Ivashkevich A, Redon CE, Nakamura AJ, Martin RF, Martin OA, Use of the γ-H2AX assay to monitor DNA damage and repair in translational cancer research. Cancer Lett. 2012 Dec 31;327(1-2):123-33.

[10] Rothkamm K, Löbrich M, Evidence for a lack of DNA double-strand break repair in human cells exposed to very low x-ray doses. Proc. Natl. Acad. Sci. USA, 2003 Apr 29;100(9):5057-62.

[11] Bonner WM, Redon CE, Dickey JS, Nakamura AJ, Sedelnikova OA, Solier S, Pommier Y, GammaH2AX and cancer. Nat Rev Cancer, 2008 Dec;8(12):957-67.

[12] Garty G, Chen Y, Turner H, Zhang J, Lyulko O, Bertucci A, Xu Y, Wang H, Simaan N, Randers-Pehrson G, Yao YL, Brenner DJ, The RABiT: A Rapid Automated Biodosimetry Tool For Radiological Triage. II. Technological Developments. Int J Radiat Biol, 2011 May 11;87(8):776–790.

[13] Wang J, Fan Z, Zhao Y, Song Y, Chu H, Song W, Song Y, Pan X, Sun Y, Li D. A new hand-held microfluidic cytometer for evaluating irradiation damage by analysis of the damaged cells distribution. Sci Rep. 2016 Mar;6:23165.

[14] Lee Y, Wang Q, Shuryak I, Brenner DJ, Turner H. Development of a high-throughput γ-H2AX assay based on imaging flow cytometry. Radiat Oncol. 2019 Aug;14(1):150.

[15] Wang Q, Lee Y, Shuryak I, Canadell MP, Taveras M, Perrier JR, Bacon BA, Rodrigues MA, Kowalski R, Capaccio C, Brenner DJ, Turner HC. Development of the FAST-DOSE assay system for high-throughput biodosimetry and radiation triage. Sci Rep. 2020;10(1):12716.

[16] Davis F, Il'yasova D, Rankin K, McCarthy B, Bigner DD. Medical diagnostic radiation exposures and risk of gliomas. Radiat Res. 2011 Jun;175(6):790-6.

[17] Lin EC. Radiation risk from medical imaging. Mayo Clin Proc. 2010 Dec;85(12): 1142-6.

[18] Dauer LT, Zanzonico P, Tuttle RM, Quinn DM, Strauss HW. The Japanese tsunami and resulting nuclear emergency at the Fukushima Daiichi power facility: technical, radiologic, and response perspectives. J Nucl Med. 2011 Sep;52(9):1426-1432.

[19] Wu TH, Chen Y, Park SY, Hong J, Teslaa T, Zhong JF, Carlo DD, Teitell MA, Chiou PY. Pulsed laser triggered high speed microfluidic fluorescence activated cell sorter. Lab Chip. 2012 Feb;12(7):1378-1383.

[20] Gonzalez CF, Remcho VT. Harnessing dielectric forces for separations of cells, fine particles and macromolecules. J Chromatogr A. 2005 Jun;1079(1-2):59-68.

[21] Mizuno M, Yamada M, Mitamura R, Ike K, Toyama K, Seki M. Magnetophoresis-integrated hydrodynamic filtration system for size- and surface marker-based two-dimensional cell sorting. Anal Chem. 2013 Aug;85(16):7666-73.

[22] Yamada M, Seki M. Hydrodynamic filtration for on-chip particle concentration and classification utilizing microfluidics. Lab Chip. 2005 Nov;5(11): 1233-9.

[23] Huang LR, Cox EC, Austin RH, Sturm JC. Continuous particle separation through deterministic lateral displacement. Science. 2004 May;304(5673): 987-90.

[24] Arosio P, Müller T, Mahadevan L, Knowles TPJ. Density-gradient-free microfluidic centrifugation for analytical and preparative separation of nanoparticles. Nano Lett. 2014 May;14(5): 2365-71.

[25] McFaul SM, Lina BK, Ma H. Cell separation based on size and deformability using microfluidic funnel ratchets. Lab Chip. 2012 Jul;12(13): 2369-76.

[26] Li M, Muñoz HE, Goda K, Carlo DD. Shape-based separation of microalga Euglena gracilis using inertial microfluidics. Sci Rep. 2017 Sep;7:10802.

[27] Jackson JM, Taylor JB, Witek MA, Hunsucker SA, Waugh JP, Fedoriw Y, Shea TC, Soper SA, Armistead PM. Microfluidics for the detection of minimal residual disease in acute myeloid leukemia patients using circulating leukemic cells selected from blood. Analyst. 2016;141(2):640-651.

[28] Farahinia A, Zhang WJ, Badea I. Novel microfluidic approaches to circulating tumor cell separation and sorting of blood cells: A review. J Sci Adv Mater Devices. 2021 Sep;6(3):303-320.

[29] Gorkin R, Park J, Siegrist J, Amasia M, Lee BS, Park JM, Kim H, Kim M, Madou M, Cho YK. Centrifugal microfluidics for biomedical applications. Lab Chip. 2010 Jul;10(14): 1758-73.

[30] Ukita Y, Oguro T, Takamura Y. Density-gradient-assisted centrifugal microfluidics: an approach to continuous-mode particle separation. Biomed Microdevices. 2017

Apr;19(2):24.
[31] Wang C, Fu Y, Guo J. An automatic whole blood analyzer for renal function analysis with a centrifugal microfluidic device. Analyst. 2022 Oct;147(21):4804-4814.
[32] Shamloo A, Naghdloo A, Besanjideh M. Cancer cell enrichment on a centrifugal microfluidic platform using hydrodynamic and magnetophoretic techniques. Sci Rep. 2021 Jan;11(1):1939.
[33] Xia Y, Whitesides GM. SOFT LITHOGRAPHY. Annu Rev Mater Sci. 1998 Aug;28: 153-184.
[34] Bhattacharya S, Datta A, Berg JM, Gangopadhyay S. Studies on Surface Wettability of Poly(Dimethyl) Siloxane (PDMS) and Glass Under Oxygen-Plasma Treatment and Correlation With Bond Strength. J Microelectromech Syst. 2005 Jul;14(3): 590-597.
[35] Xu L, Lee H, Jetta D, Oh KW. Vacuum-driven power-free microfluidics utilizing the gas solubility or permeability of polydimethylsiloxane (PDMS). Lab Chip. 2015 Sep;15(20)
[36] Scott MD, Matthews K, Ma H. Current and Future Aspects of Nanomedicine. IntechOpen; London, UK: 2019. Assessing the Vascular Deformability of Erythrocytes and Leukocytes: From Micropipettes to Microfluidics. 2019 Nov
[37] Milisavljević J, Petrović E, Ćirić I, Mančić M, Marković D, Đorđević M. TENSILE TESTING FOR DIFFERENT TYPES OF POLYMERS. Conference: 29th Danubia – Adria Symposium on Advances in Experimental Mechanics. 2012 Sep

Data Availability Statement

Raw data were generated at Ibaraki university and Gunma university. Derived data supporting the findings of this study are available from the corresponding author Kenta Takahashi on request.